Spray quality at elevated gas densities via swirl and air-assisted atomisation methods

H. Lienemann, J.S. Shrimpton and J.T. Kashdan*

Imperial College
Dept. of Mechanical Engineering
Exhibition Road
London SW7 2BX
UK

*Stanford University
Dept. of Mechanical Engineering
Duena Street
Stanford, Ca
USA

Abstract

We investigate the changes in spray character generated by two potential atomizer designs that are under consideration for use in Direct Injection Spark Ignition (DISI) engines. The two atomizers are the more usual pressure swirl and the air assist design. Sprays of each atomizer are investigated in a constant volume chamber for conditions corresponding to early and late injection in DISI engines using imaging and Phase Doppler Anemometry (PDA). The application of these techniques reveals that the mean drop size increases as ambient gas density is increased for both atomiser designs, which suggests that the air assist atomizer also has some form of liquid sheet that disintegrates to form droplets. This implies that both atomizer types, if used during the compression stroke, will encounter evaporation rate constraints.

Introduction

In DISI engines as compared to port fuel injected (PFI) engines, there is a much greater emphasis on the mixture preparation stage because of the shorter timescales available to produce an ignitable mixture at the time of ignition. This applies in particular to DISI engines under stratified operation where fuel must be injected shortly before the time of ignition i.e. late in the compression stroke. The main problems related to injection and subsequent combustion under these conditions are high engine-out HC and NO_X emissions as well as soot emissions. It has been reported in previous studies on various DISI engine concepts that the mixture preparation time, the time from start of injection till ignition, is strongly influential on these emissions [1, 2]. The fuel injection system should for any given in-cylinder gas density therefore produce droplets small enough to allow for sufficient droplet heat up, evaporation and air/fuel mixing. There are currently two principal ways of injecting fuel in DISI engines: single fluid, high-pressure injection and dual fluid, low-pressure injection. Single fluid injection systems operate at fuel pressures of between 50 and 120 bars with injection duration

times in the range of 0.5 to 4.5 ms [3]. Single fluid pressure-swirl atomisers (PS-atomisers) have been adopted by the engine industry [4, 5] due to their nominally fine atomisation and wide spray dispersal. There have been a number of analytical [6, 7] and experimental [8] studies relating to the break-up of the liquid sheet and droplet formation whilst further experimental studies have focused on the spray characteristics [9]. Dual fluid systems employ a sequenced pair of injectors in which air first pressurises a mixing chamber before the fuel-metering event begins. This two-phase charge resides for a short delay period before being injected into the combustion chamber. Air pressures of 6 to 10 bar and differential air/fuel pressures of ~1 bar are employed with charge injection duration times of 4 to 7 ms [3]. Many experimental and analytical studies have been carried out focusing on the operating parameters and spray characteristics of air-assisted atomisers (AA-atomisers) and their application in DISI engines [10, 11, 12]. The work described here focuses on the comparison of PS- and AA-atomisers in order to examine the performance of both injectors in DISI engines and specifically their response to elevated ambient pressures characteristic of a late injection strategy in a typical DISI engine.

Experimental Set-up

The AA-atomiser is made of an assembly of a PFI fuel injector running at 9 bars and an air injector running at 7.5 bars absolute pressure. For the application in DISI engines these parameters are generally chosen as the best compromise between indicated fuel consumption and parasitic losses over the full engine speed/load range [10]. A compressed air bottle and two electrical fuel pumps provided the required air and fuel flow respectively. The constant volume chamber (CVC) test rig, the PS-atomiser test rig, the imaging system and the PDA system were the same as previously described by Kashdan et al. [14].

Table1: Ambient gas test conditions

Injection strategy	Adiabatic compression [bar, ˚C, kg/m^3]	CVC conditions [bar, ˚C, kg/m^3]	
		AA	PS
'early'	p_{ch}= 1, T_{ch}= 70, ρ_{ch}=1	p_{ch}= 1, T_{ch}= 20, ρ_{ch}= 1	p_{ch}= 1, T_{ch}=20, ρ_{ch}= 1
'mid'	p_{ch}= 3, T_{ch}=150, ρ_{ch}=3	p_{ch}= 4, T_{ch}=165, ρ_{ch}= 3	p_{ch}= 5, T_{ch}=20, ρ_{ch}= 5
'late'	p_{ch}=10, T_{ch}=350, ρ_{ch}=6	p_{ch}= 4, T_{ch}= 20, ρ_{ch}= 5	p_{ch}= 7, T_{ch}=20, ρ_{ch}= 8

In all tests, gasoline has been replaced by iso-octane (trimethyl-pentane 2,2,4) and the fuel delivery rate was 13 mg/injection for both injectors. Both injectors were found to have an inherent delay between the electrical start, defined by the rising edge of a TTL pulse and the emergence of liquid of approximately 0.27ms for the PS atomizer and 1.2 ms for the AA-atomiser. The electromechanical delay was found to vary slightly with P_{inj}, from 0.24ms at 20 bars to 0.27ms at 100 bars for the PS-atomiser [13] and 1.2ms at 1bar to 1.3ms at 5bar for the AA- atomiser. The injection pressure and injection duration were kept constant at 80 bars and 1.5ms for the PS-atomizer in all cases. For the AA injector the timings were fixed at 3.3ms for the fuel pulse width, 3.7ms for the air pulse width and 2.2ms for the fuel-air delay.

Comparison of Spray Characteristics

It was shown in previous experimental spray investigations [13, 14], that visualization studies reveal the spray to be axisymmetric on a macroscopic level and the images taken have shown this to be the case for sprays from these particular injectors. Traversing the PDA radially across the spray performed a further verification of the spray symmetry. Figures 1 and 2 show sequences of split images (PS-atomiser to the left, AA-atomiser to the right) at four time windows (Δt=0.5ms) overlaid with local axial mean and rms droplet velocity and size information obtained from PDA measurements. The PDA data was processed into 0.1 ms time intervals. The sequence in Fig. 1 corresponds to 'early' injection conditions and the sequence in Fig. 2 corresponds to 'late' conditions. For interpretation of these pictures it should be noted that the PS-atomiser not only injects the same amount of fuel in a shorter period of time as compared to the AA-atomiser but also exhibits a much shorter response time as mentioned earlier. In order to allow for a direct comparison of both sprays, each sequence of split images (grayscale reduced to 4 bit) in Fig. 1 and 2 was referenced to a specific point in time t_{rel} for each injector relative to the start of injection. This point in time corresponds to the end of the specific injection duration Δt_{inj} including the specific injector delay time Δt_{delay} referenced from the electrical start of injection t_{esoi} (rising edge of TTL pulse): $t_{rel}=t_{esoi}+\Delta t_{inj}+\Delta t_{delay}$. For the AA-atomiser t_{rel} calculates to $t_{rel}=t_{esoi}$+3.7ms+1.25ms=4.95ms for the PS-atomiser t_{rel} calculates to $t_{rel}=t_{esoi}$+1.5ms+0.25ms=1.75ms.

It is clear from Fig. 1 that both injectors produce a significantly different spray in terms of global shape and rate of penetration. The spray produced by the PS-atomizer is typical, consisting of a characteristic 'pre-spray' that is well ahead of the main spray, as identified from Fig. 1(a). The pre-spray is associated mainly with droplets of about 60µm diameter but parts of the pre-spray are known to consist of much larger droplets. Axial velocities range from 55 to 65 m/s. The main spray itself appears as a cone which eventually widens up to form an 'umbrella' structure as shown on the next sequential images.

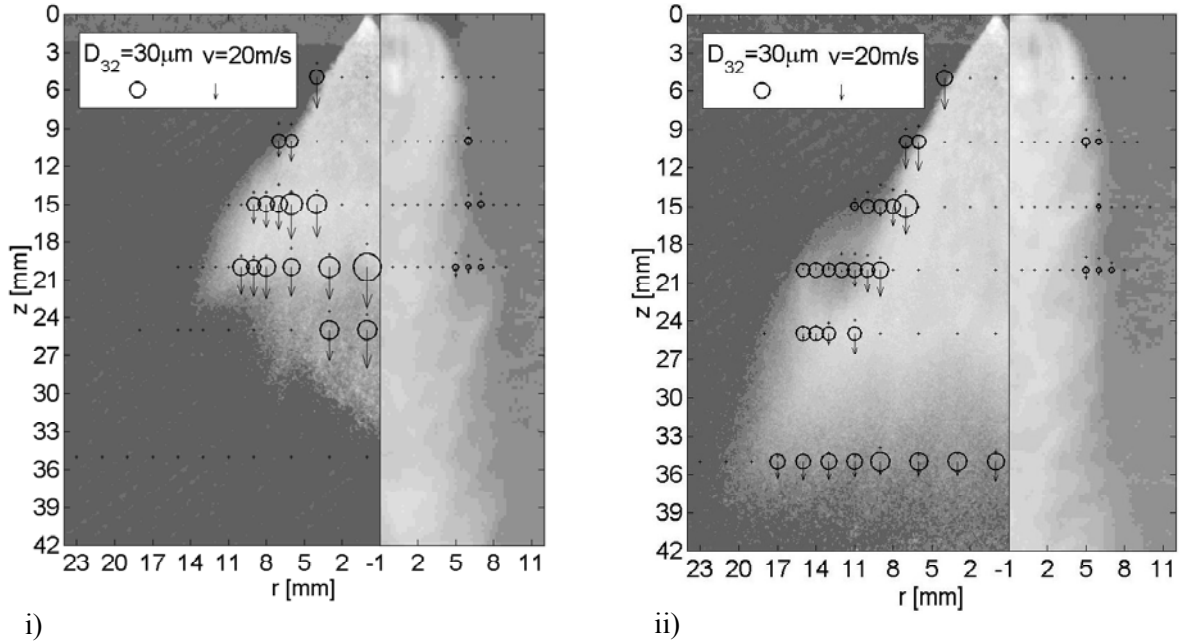

Figure 1a: Sequential spray images for PS- and AA-atomiser, 'early' injection conditions, droplet diameter D_{32} (circles), mean axial velocities (vectors), axial rms velocities (crosses), 'early' injection conditions (p_{ch}=1bar, T_{ch}=20ºC) for i) t_{rel}=-1.0ms, ii) t_{rel} =-0.5ms

This ‘umbrella’ shape is formed by a toroidal vortex consisting of droplets with a diameter range of 15 to 30µm and negative axial velocity. At the same time t_{rel} the spray of the AA-atomiser appears in a shape more similar to a gas jet. The spray plume is about twice as long as the PS-atomiser spray for the atmospheric test case with a comparably high reduction in axial penetration as the ambient pressure increases and the driving force for the spray process is reduced (Fig. 2). In terms of PDA data less information is available due to the structure of the spray especially for the spray core. However, data obtained from the edge of the AA-spray show a significantly lower mean diameter of droplets than for the PS-spray. It is only after approximately t_{rel}=0.5ms that larger droplets were detected for the AA-spray.

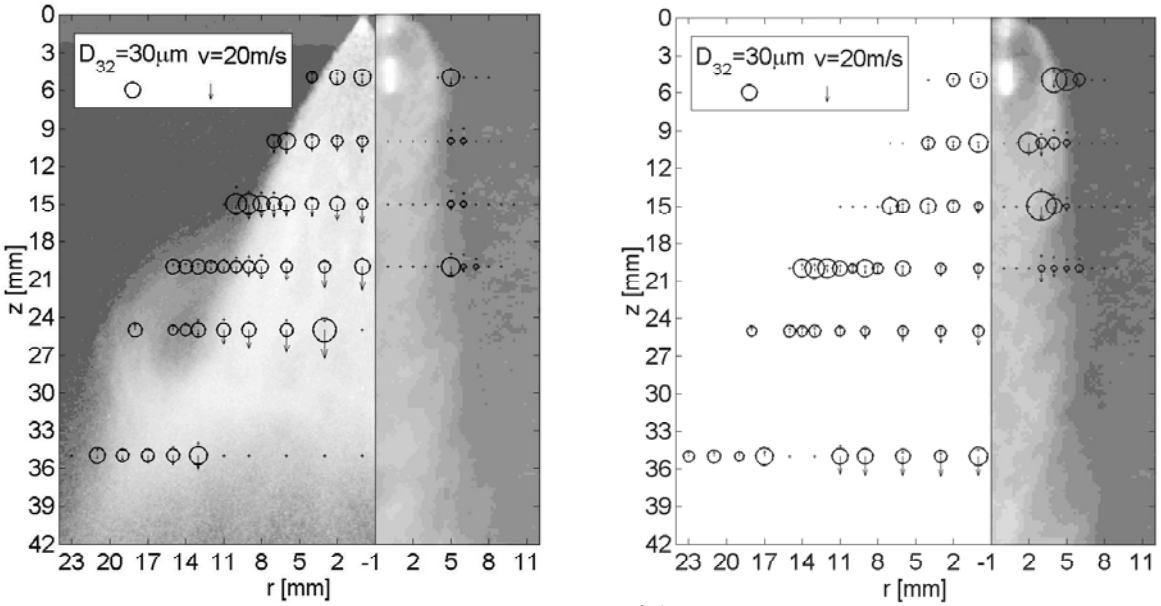

iii) iv)

Figure 1b: Sequential spray images for PS- and AA-atomiser, ‘early’ injection conditions, droplet diameter D_{32} (circles), mean axial velocities (vectors), axial rms velocities (crosses), ‘early’ injection conditions (p_{ch}=1bar, T_{ch}=20ºC) for iii) t_{rel} =0ms, iv) t_{rel} =0.5ms

The elevated gas density suppresses the mean axial velocity and hence the axial spray penetration as illustrated in Fig. 2. Penetration rate data extracted from images for the PS-atomiser reveal that the spray velocities in the near nozzle region were in the range of 50 to 70 m/s for atmospheric chamber conditions and 30 to 40 m/s for 7bar. PDA measurements have also confirmed this. The initial penetration rate shortly after t_{esoi} for the AA-atomiser was found to be in the range of 50 to 60 m/s for the atmospheric case and 20 to 30 m/s for elevated pressure. These data also compare favourably with data obtained during studies for similar AA-atomiser test rigs (e.g. [10]) and PS-atomiser test rigs (e.g. [15]). The droplet sizing information available for the spray edge for both atomiser types suggests an increase in droplet diameter in both sprays.

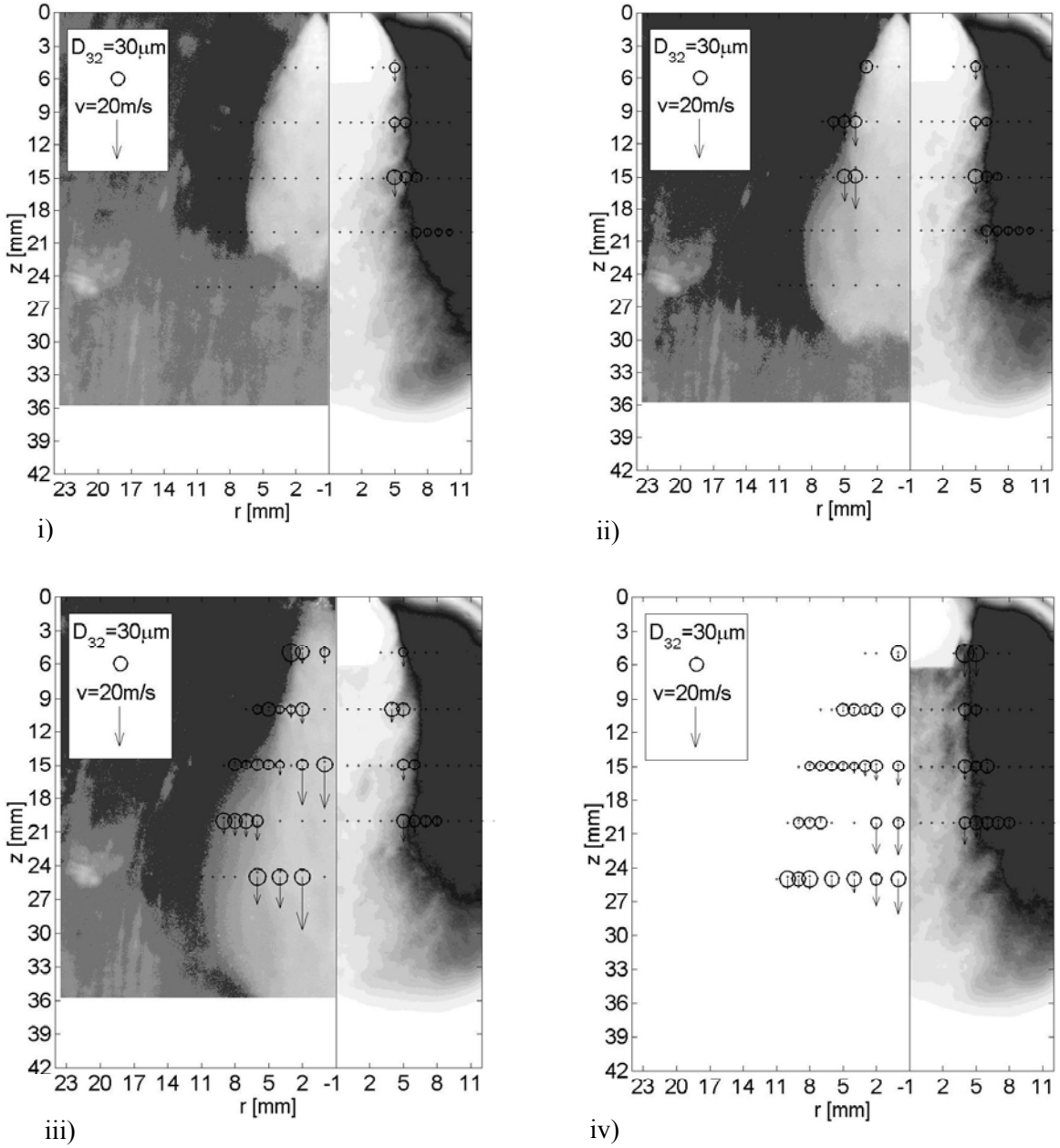

Figure 2: Sequential spray images for PS- and AA-atomiser, droplet diameter D_{32} (circles), mean axial velocities (vectors), axial rms velocities (crosses), 'late' injection conditions (p_{ch}=1bar, T_{ch}=20ºC) for i) t_{rel}=-1.0ms, ii) t_{rel} =-0.5ms, iii) t_{rel} =0ms, iv) t_{rel} =0.5ms

Temporal plots of PDA results obtained at locations z=25mm/r=0mm and z=20mm/r=0mm (relative to the injector nozzle) corresponding to the injector centerline and at z=25mm/r=8mm and z=20mm/r=4mm corresponding to the spray edge are presented in Fig. 3 and 4 for chamber pressures of 1, 5 and 7 bars. Temperatures inside the CV-chamber were kept constant at room temperature except for one AA-atomiser test series, which was carried out at p_{ch}=4bar and T_{ch}=165ºC. However, the elevated temperature has only a limited effect on the droplet size information due to the droplet heat up and evaporation times involved. The discrete velocity and size data were processed into bins of 0.1ms width. In the case of the PS-atomiser and for the time interval of -0.5ms< t_{rel}<0ms attenuation of both the

incident and scattered light caused by the dense spray cone makes valid measurements extremely difficult on the injector centreline as reported previously [13].

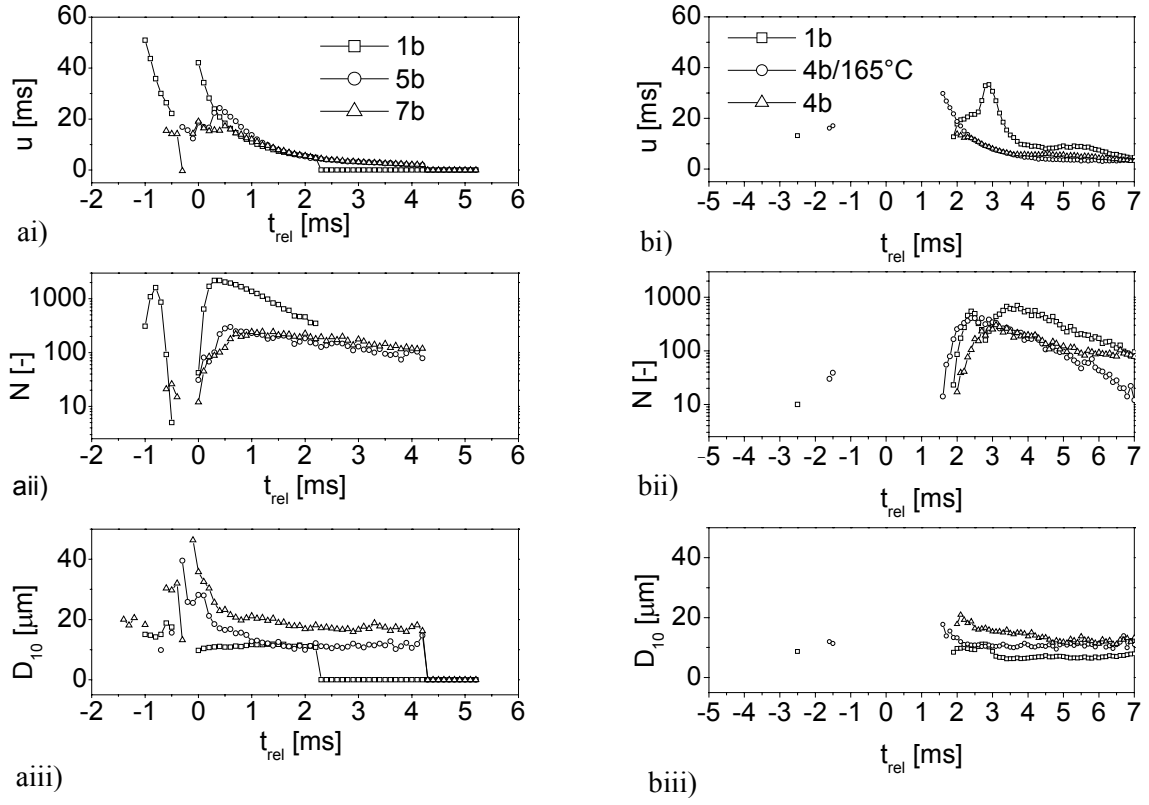

Figure 3: Time resolved PDA data at injector center line for a) PS-atomiser at z=25mm and b) AA-atomiser at z=20mm, showing i) mean axial velocities, ii) valid sample counts and iii) arithmetic mean diameter

For t_{rel}>0ms the trailing edge of the spray is measurable with velocities decreasing monotonically thereafter. The droplet sizes measured within the pre-spray for p_{ch} =1bar range from 15µm<D_{10}<17µm. In contrast, for p_{ch}=7bar the mean diameters at this location are significantly larger, in the range of 30 µm<D_{10}<33µm for -0.6ms<t_{rel}<-0.4ms. Mean droplet diameters in the main spray were measured in the range 10µm<D_{10}<12µm at 1bar ambient pressure and 18µm<D_{10}<22µm at 7bar ambient pressure. The PDA data plots for the air-assisted spray (Fig. 4) exhibit the same lack of data as for the PS-atomiser for a time interval of approximately 0ms to 5.0ms after t_{esoi}, which corresponds to the air pulse width of the injector (Δt_{inj} = 3.7 ms) and the delay time (Δt_{delay} = 1.25 ms). Thus the data in Fig. 4 represent mainly measurements in the trailing edge of the spray. Nonetheless, the data reveals for 1 bar and 4 bar conditions similar characteristics as compared to the pressure-swirl spray in terms of ambient gas density and mean droplet size correlation. Droplets measured for the atmospheric case appear in the range of 6µm<D_{10}<10µm. In contrast, for p_{ch}=4bar the mean diameter at the same location is significantly larger in a range between 14µm<D_{10}<20µm.

We investigated further other locations where PDA data was obtained for both atomisers and the range of chamber conditions. An example is provided in Fig. 4 for a position nearer the spray edge (z=25mm/r=8mm for the PS-atomiser, z=20mm/r=4mm for the AA-atomiser). It is demonstrated that the sensitivity of mean diameter to ambient density is indeed a macroscopic spray feature and not due to fine scale structuring of the spray because of the specific

atomizer characteristic. The range of mean droplet sizes change for the PS-atomiser from $15\mu m<D_{10}<20\mu m$ (1bar) to $18\mu m<D_{10}<25\mu m$ (7bar) and for the AA-atomiser from $8\mu m<D_{10}<10\mu m$ (1bar) to $15\mu m<D_{10}<20\mu m$. Figure 3 and 4 suggest that there is a correlation between mean droplet diameter and ambient gas density for both of the atomisers of the form

$\frac{D_{10}(\rho_2)}{D_{10}(\rho_1)} = A \times \frac{\rho_2}{\rho_1}$, where A is approximately 0.2 (PS-atomiser) and 0.4 (AA-atomiser).

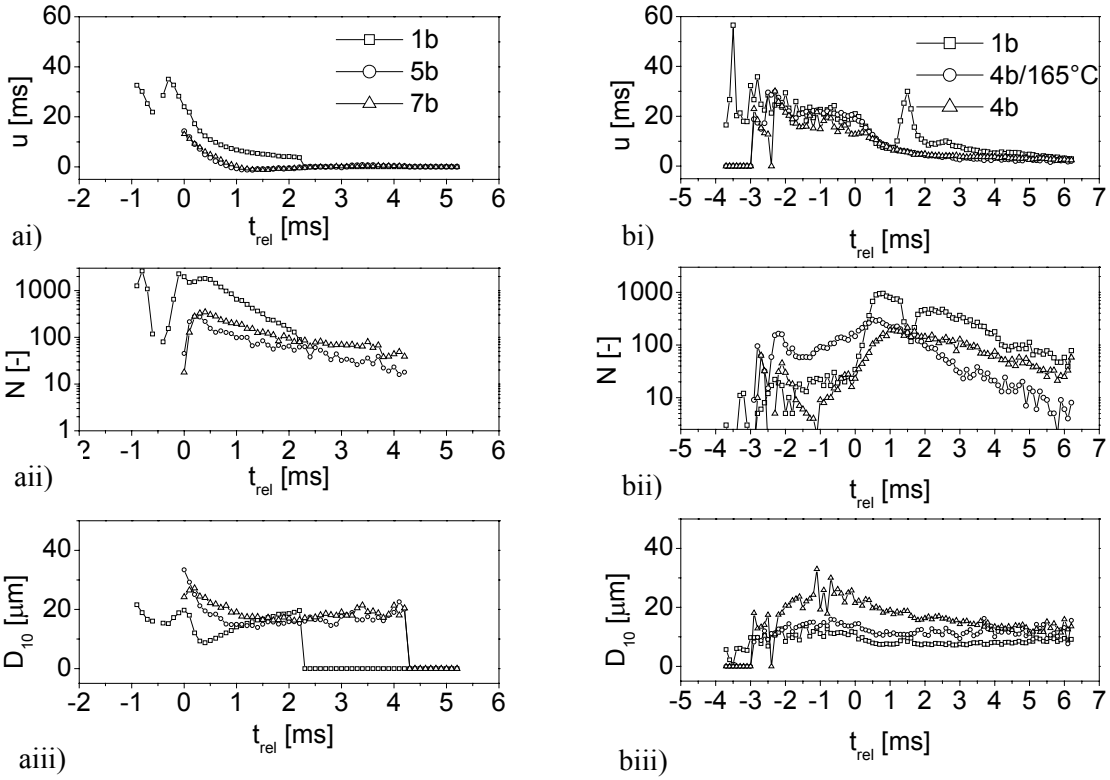

Figure 4: Time resolved PDA data near sprayedge for a) PS-atomiser at z=25mm/r=8mm and b) AA-atomiser at z=20mm/r=4mm, showing i) mean axial velocities, ii) valid sample counts and iii) arithmetic mean diameter

De Corso was among the first to investigate the influence of ambient air pressure on the spray characteristics of PS-atomisers in the 1960's also measured a 38% increase in mean droplet size with a chamber pressure increase from 1 bar to 7.9 bar [16]. The factor A based on these data can be approximated by a value of 0.1 based on the Sauter mean diameter (SMD). Recent studies show the same effect for AA-atomisers [12] and PS-atomisers [18] both injecting into 1bar and 4bar ambient pressure with approximate values of A=0.3 and A=0.2 respectively. One might expect that an increase in the Weber number resulting from an increase in the air density from $1.3kg/m^3$ to $8.1kg/m^3$ for p_{ch}=1 bar and 7 bar respectively would serve to enhance atomisation quality in terms of reducing the characteristic mean droplet sizes. However, the droplet Weber number that is proportional to droplet diameter and would thus increase at the elevated chamber pressure appears to be dominated by the significant reductions in droplet velocity, which were observed. De Corso proposed that a continuing decrease in droplet size with increase in ambient pressure would be expected, since the increase in pressure gradients around the droplet surface lead to bigger drop deformation

rates. Thus as ambient pressure rises, a decrease would be expected in the critical stable droplet size. The observed *increase* in droplet size was attributed to increased coalescence of the spray droplets as the ambient pressure increased [16]. However, we suggest another explanation based upon the change in the rate of the atomisation process, which is more likely to describe the cause of the increase in droplet size at higher chamber pressures correctly: The growth rate of the surface waves that are formed in the near nozzle region of a conical liquid sheet would be intensified at higher chamber pressures and the resulting sheet break-up length would be reduced. Thus an initially thicker sheet would produce ligaments and subsequent droplets of larger characteristic sizes.

Conclusions

These findings have important implications for the adoption of atomisers for DISI engines. Whilst the atomisation performance may be sufficient for operation in the intake stroke with approximately ambient gas densities the challenge remains to employ later injection timings during the compression stroke thus exploiting part load fuel economy benefits. This problem seems to apply not only for the PS-atomiser but also for the AA-atomiser since both evidently produce larger droplets at elevated gas densities.

Acknowledgements

The authors would like to acknowledge financial support for this work from the European Union. In addition, thanks are due to Nicolas Perquis for carrying out the measurements on the air-assisted atomiser test rig.

References

[1] H. Sandquist 2000 *SAE Technical Paper Series* 2000-01-1906
[2] H. Sandquist 1998 *SAE Technical Paper* 982701
[3] G. Wigley 1999 ILASS-Europe
[4] Y. Iwamoto et al. 1997 *SAE Technical Paper Series* 970541
[5] J. Harada et al. 1997 *SAE Technical Paper Series* 970540
[6] Z. Han et al. 1997 *Atomization and Sprays* **7** 663-684
[7] D. Schmidt et al. 1999 *SAE Technical Paper Series* 1999-01-0496
[8] T. Okamoto et al. 1998 *Trans. ASME* **120** 586-592
[9] C. Jang et al. 2000 *Atomization and Sprays* **10** 159-178
[10] G. Cathcart et al. 2000 *SAE Technical Paper Series* 2000-01-0256
[11] G. Cathcart et al. 2001 *JSAE Technical Paper Series* 20015360
[12] C. Jang et al. 2000 *Atomization and Sprays* **10** 199-217
[13] J. Kashdan et al. *Atomization and Sprays*, accepted for publication
[14] J. Kashdan 2002 PhD Thesis Imperial College London
[15] L. Araneo et al. 2000 *SAE Technical Paper Series* 2000-01-1901
[16] S. DeCorso 1960 Trans. *ASME Jour. Eng. Power* **82** 10-18
[17] G. Maier 1998 *SAE Technical Paper Series* 982523
[18] P. Williams, S. O'Donoghue, R. Anderson and S. Richardson 2001 *SAE Technical Paper Series* 2001-01-1974